Vertical Crystallization of C_{60} Nanowires by Solvent Vapor Annealing Process

Jungah Kim, Chibeom Park, Ji Eun Park, Kwangho Chu, and Hee Cheul Choi*

Department of Chemistry, Pohang University of Science and Technology (POSTECH), San 31, Hyoja-Dong, Nam-Gu, Pohang, Korea 790-784

ABSTRACT We report that C_{60} molecules are spontaneously crystallized into vertical nanowires by the solvent vapor annealing (SVA) process. C_{60} molecules have been known to be assembled into wire-like crystals by simply dropping and drying C_{60} solutions in *m*-xylene on a solid substrate. By the drop-drying process, C_{60} nanowires have been mostly grown laterally on a solid substrate, as the major force applied to the droplet during the drying process is parallel to the substrate. On the other hand, the SVA process seems to provide an ideal environment under which the direction of the dominant drying force of a droplet becomes vertical. When a thermally evaporated C_{60} film is exposed to *m*-xylene solvent vapor under controlled SVA environments at room temperature, C_{60} molecules are found to be crystallized into vertical nanowires. The effect of solvent vapor pressure on the vertical growth of C_{60} nanowire is examined by comparative studies using mesitylene and 1,3-dichlorobenzene. The versatility of the SVA process for the growth of vertical organic nanostructures is further demonstrated by the successful formations of vertically grown C_{60} 2D disks and 5,7,12,14-pentacenetetrone anisotropic crystals by employing carbon tetrachloride and toluene solvent vapors, respectively.

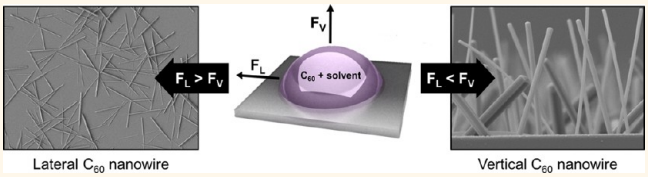

KEYWORDS: fullerenes · self-crystallization · solvent vapor annealing · vertical growth · organic crystal

The development of efficient growth methods for the low-dimensional organic crystals composed of highly conjugated molecules provides opportunities to design new soft building blocks of which properties are largely different from those observed from powder or solution phase.[1−6] One approach being explored again recently is to utilize spontaneous precipitation in solution phase that involves self-crystallization of target molecules at liquid−liquid,[7] liquid−air,[8] or liquid−air−solid interfaces.[9,10] Especially, crystallization at the liquid−air−solid interface that can be achieved by a simple process, called the drop-drying process, has recently attracted much attention due to its simplicity of experimental setup as well as high efficiency in terms of yield and reaction time. For example, C_{60} molecules are readily crystallized by the drop-drying process into 0D, 1D, and 2D C_{60} nano- to microstructures at room temperature by simply dropping C_{60} solutions containing geometry-determining solvents.[11] Although the drop-drying process is an efficient way to form geometrically well-defined C_{60} crystals, one important drawback that has not been resolved yet is the controllability of growth direction.

Despite its importance, the vertical crystallization of conjugated molecules has been reported only for limited examples including peptides,[12−16] 1,5-diaminoanthraquinone,[17−19] and copper phthalocyanine.[20] Except the aromatic dipeptide nanotubes (ADNTs) that have been vertically grown by the action of fast evaporating solvent,[12] all other examples require either a high temperature, template, or physical vapor transport environment. Although a few examples of occasionally obtained C_{60} nanowires grown on the wall of reaction vials or at the edges of substrates have witnessed the possibility of template-free vertical growth of C_{60} nanowires,[21] it is still demanding to develop growth methods that grant specific and spontaneous formation of vertical C_{60} nanowires in high yields in a controlled manner. Herein we report that C_{60} molecules are successfully crystallized into high-yield vertical nanowires by the solvent vapor annealing (SVA) process at room temperature. SVA was first introduced for harnessing thermally unstable polycrystalline organic thin films to supersede the

* Address correspondence to choihc@postech.edu.

Received for review July 19, 2013 and accepted September 9, 2013.

Published online September 09, 2013
10.1021/nn403729g

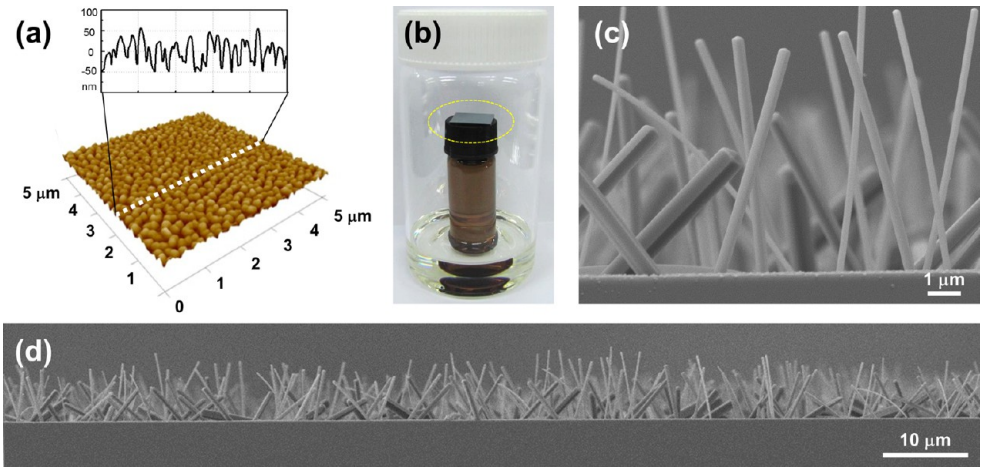

Figure 1. (a) AFM image of thermally evaporated C_{60} film. (b) Photograph of the SVA apparatus. (c, d) High- and low-magnification SEM images of vertically crystallized C_{60} nanowires on a Si substrate, respectively.

thermal annealing process.[22,23] While the original role of SVA has been focused mainly on the enhancement of crystallinity of organic films, its unveiled capability to form organic molecules into specific geometrical structures directly on solid substrates has recently attracted much attention, especially regarding the growth of organic single crystals in mild conditions.[24−26] In this article, we demonstrate that the SVA process provides an ideal environment to assemble C_{60} molecules in the vertical direction by utilizing the action of solvent molecules evaporating along the direction normal to the substrate. Such an action of solvent evaporation that determines the direction of crystallization has been confirmed by verifying the same growth tendencies with various solvents having different vapor pressures. The versatility of the SVA process for vertical growth is also demonstrated by the vertical growth of C_{60} disks and 5,7,12,14-pentacenetetrone (PT) anisotropic crystals.

RESULTS AND DISCUSSION

The SVA process was conducted by placing a Si substrate containing a thermally evaporated C_{60} film (Figure 1a, average thickness of 60 nm) in a scintillation vial filled with 5 mL of *m*-xylene solvent (Figure 1b). Note that *m*-xylene is the solvent known to guide C_{60} molecules into being crystallized into lateral nanowires by the conventional drop-drying process.[9,11,27,28] To avoid direct contact between the C_{60} film and *m*-xylene, the sample was placed on top of an inner pillar taller than the level of solvent. The vial was then capped to keep the sample under constant vapor pressure of *m*-xylene at 28 °C, which allows natural coverage of the C_{60} film with *m*-xylene vapor enough to wet C_{60} molecules and to evaporate the solvent under dynamic equilibrium. Upon 12 h of the SVA process, C_{60} molecules are crystallized in the vertical direction as shown in Figure 1c. The average diameter and length of vertical C_{60} nanowires grown under this condition are about 340 nm and 7 μm, respectively. The formation of a vertical C_{60} nanowire is highly reproducible with high homogeneity, as evidenced by the large-area cross-section SEM image (Figure 1d).

The structure of C_{60} nanowires was characterized based on Raman spectroscopy, powder X-ray diffraction (XRD), and selected area electron diffraction (SAED) data. The inclusion of *m*-xylene in the vertically grown C_{60} nanowires was first confirmed by Raman spectroscopy, as the presence of solvent molecules in the C_{60} nanowire is supposed to shift Raman peaks of $H_g(1)$ mode and $A_g(1)$ mode.[9,28,29] While solvent-free C_{60} crystals usually have a cubic crystal system, it has been known that a hexagonal crystal system is preferred when C_{60} molecules are cocrystallized with solvent molecules as they are incorporated at the interstitial sites of C_{60} crystals.[27,30] Indeed, the vertically grown C_{60} nanowires show $H_g(1)$ mode Raman peak shifts from 272 to 270 cm^{-1} and $A_g(1)$ mode from 496 to 494 cm^{-1}, compared with pristine C_{60} powder (Figure 2a). This result confirms that the vertically grown C_{60} nanowires are solvated with *m*-xylene.

Next, the crystal structure of vertically grown C_{60} nanowires is assigned using XRD and SAED data. The XRD patterns were obtained from two samples obtained from the same batches, but prepared differently for XRD measurement purposes: one is an as-grown sample containing vertically aligned C_{60} nanowires, and the other one is the sample containing C_{60} nanowires laying down on a substrate by mechanically pressing down the vertical nanowires at slightly off-angle using a glass slide. The XRD pattern from the as-grown sample shows three distinct diffraction peaks at 2θ larger than 18, *i.e.*, at 19.250, 20.833, and 21.541, which correspond to (041), (231), and (141) planes, respectively. Very weak diffraction from the (010) plane and the absence of diffraction peaks from (*hk*0) planes appearing at low 2θ values is due to the vertical alignment of C_{60} nanowires. On the other hand, the

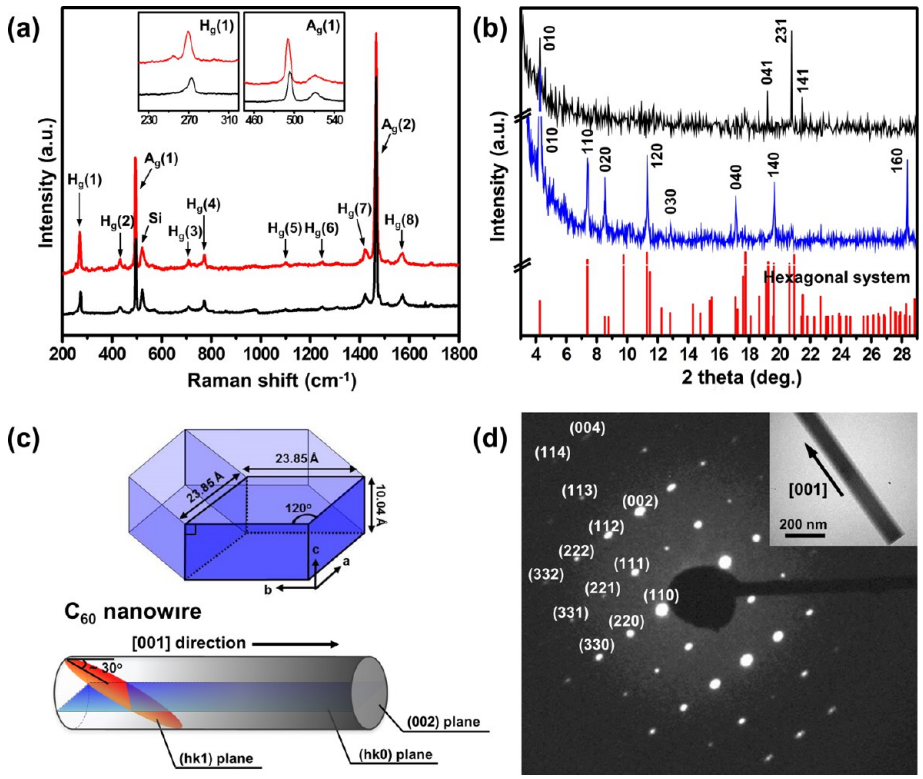

Figure 2. (a) Raman spectra of C_{60} powder (black) and vertical C_{60} nanowires (red). Insets are magnified views for $H_g(1)$ and $A_g(1)$ regions. (b) XRD patterns of as-grown vertical C_{60} nanowires (top), mechanically laid down vertical C_{60} nanowires (middle), and simulation data. (c) Unit cell of a hexagonal system with calculated lattice parameters (top) and schematic depicting crystal growth axis and planes of C_{60} nanowire. (d) SAED pattern of a vertical C_{60} nanowire (shown in inset).

XRD pattern obtained from the other sample containing lateral C_{60} nanowires shows eight sharp diffraction peaks at 2θ values of 4.278, 7.388, 8.557, 11.321, 12.866, 17.157, 19.705, and 28.454, which are assigned to the (010), (110), (020), (120), (030), (040), (140), and (160) planes, respectively (Figure 2b). These results matched the patterns observed from previously reported *m*-xylene-solvated C_{60} crystals having a hexagonal crystal system with the $P6_3$ space group.[31] The unit cell parameters are calculated to be a = 23.85 Å and c = 10.04 Å (a/c = 2.375, Figure 2c), which are slightly different from the reference values (a = 23.69 and c = 10.05 Å) that were obtained at 100 K. Nevertheless, the indexing of the hexagonal system for the vertical C_{60} nanowires stands correct, as the simulation result (bottom data in Figure 2b) calculated based on the $P6_3$ space group using the obtained lattice parameters matched well with both experimental results (top and middle data in Figure 2b).[32]

The SAED pattern obtained from a C_{60} nanowire shown in the inset of Figure 2d confirms that the C_{60} nanowire is single crystalline with a zone axis of [1−10] and crystal growth axis of [001], which agrees with a simulated SAED pattern as well (Figure S1 in the Supporting Information).[32] It should be noted that the electron diffraction from the (002) planes from a single C_{60} nanowire is prominent because the (002) planes are parallel to the zone axis, but the XRD peak from (002) is almost absent because of the relatively small effective area of the (002) planes for X-ray diffraction (Figure 2c), similar to the case of laterally grown C_{60} nanowires by the drop-drying method (Figure S2 in the Supporting Information).[11,27,28]

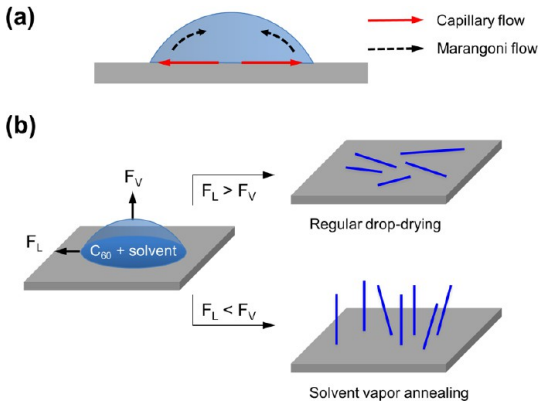

Scheme 1. (a) Two main flows generated in the droplet during evaporation of solvent. (b) Schematic representation of lateral (F_L) and vertical (F_V) forces applied to a droplet during the drop-drying process.

The most critical environment for the growth of vertical C_{60} nanowires is to control the main direction of solvent movement to be vertical (Scheme 1). The edges of a droplet containing solutes are pinned on a surface in general cases of the drying process; thus capillary outward flow is naturally generated inside the droplet to replenish solvents to the perimeter of the

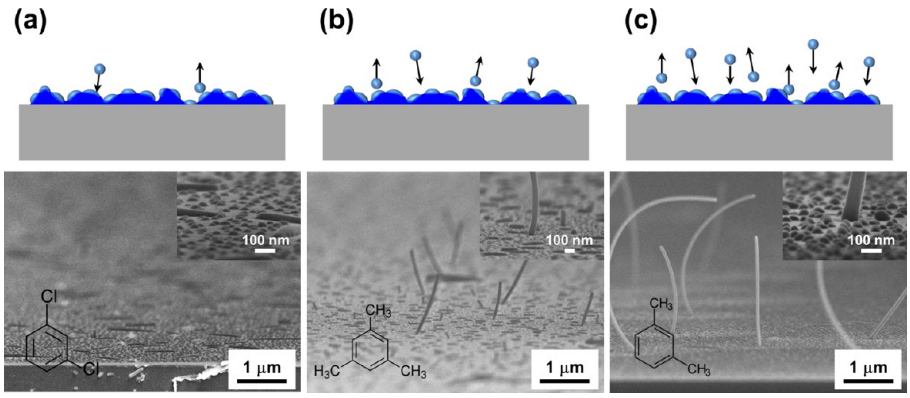

Figure 3. SEM images of C_{60} nanowires grown by the SVA process attempted with (a) 1,3-dichlorobenzene, (b) mesitylene, and (c) *m*-xylene. Qualitative expressions for the relative degree of solvent wetting on C_{60} film and the number of solvents involved during the evaporation are schematically depicted.

droplet.[33] If there are thermal and concentration gradients, circulating flow (which is also called Marangoni flow) is also generated and competes with the capillary flow (Scheme 1a).[33] Due to such capillary flow, the solutes in the droplet are accumulated at the edges of the droplet during the evaporation of the solvent, resulting in lines of solutes, which is called the "coffee ring effect". When the solvent has a high vapor pressure, as in the case of C_{60} in *m*-xylene solution, however, the droplet pinning is no longer sustained because of rapid and massive lateral expansion and shrinkage of the droplet on the surface, resulting in the crystallization of C_{60} nanowires grown laterally along the direction of solution expansion (Movie 1 in the Supporting Information). Based on this phenomenon, a simplified model for the forces applied to a macrosize droplet of C_{60} in *m*-xylene is proposed as shown in Scheme 1b. That is, in the case of the regular drop-drying process of a C_{60} solution in *m*-xylene (the diameter of the droplet is ~1 cm), the lateral force of the solvent (F_L) is dominant, resulting in laterally grown C_{60} nanowires on a substrate.

In order for vertical crystallization of C_{60} to occur, F_L should be minimized while maximizing vertical drying force of the solvent (F_V), and the SVA seems to be an ideal process to provide such an environment. The extent of F_L *versus* F_V is frequently determined by the presence or absence of coffee rings at the circumference of an original droplet upon drying as the supersaturated state is mainly formed at the three-phase contact line[34] that moves in stick−slip motions toward the inside of the droplet, affecting the direction of self-assembly.[9,10] The formation of a coffee ring indicates that F_L is larger than F_V, which can be prohibited when the droplet size becomes small enough to provide an environment where F_V becomes dominant over F_L. We confirm that the coffee ring appears when the size of a droplet of C_{60} solution in *m*-xylene is large, and it disappears when the droplet diameter becomes smaller than about 10 μm (Figure S3 in the Supporting Information).

The absence of a coffee ring upon drying indicates that F_V becomes dominative over F_L. However, as also clearly shown in Figure S3, there is no C_{60} nanowire formed in either the vertical or lateral direction because the absolute amount of C_{60} molecules in such small droplets is not enough to grow them into meaningful sizes of nanowires. Considering the successful growth of vertical C_{60} nanowires from C_{60} film under an SVA environment even without a trace of a coffee ring, the SVA process satisfies two requirements deduced from the coffee ring experiments: (1) minimization of the size of individual C_{60} droplets through continuous condensation and evaporation of solvent droplets at a couple of molecular layer thickness and (2) continuous supply of enough C_{60} molecules from C_{60} films. A phenomenon similar to the former has been recently reported by Li *et al.*, demonstrating the successive reduction of droplet size down to micrometer scale and increase of the number of droplets upon continuous evaporation and condensation for ice nucleation on a solid substrate.[35]

Since the determination of crystallization direction is also affected by the vapor pressure of solvent, which determines the number of solvent molecules in action during evaporation, control SVA experiments were attempted using mesitylene and 1,3-dichlorobenzene solvents, having different vapor pressures but known to crystallize C_{60} molecules into nanowires by the drop-drying process.[11] The vapor pressure of *m*-xylene (9.94 mmHg at 28 °C)[36] is the highest followed by those of mesitylene and 1,3-dichlorobenzene (3.09[36] and 2.02 mmHg[37] at 28 °C, respectively). Therefore, the absolute amount of solvent in action to pull solvated C_{60} molecules normal to a substrate surface is the highest for *m*-xylene and the lowest for 1,3-dichlorobenzene. To show the vapor pressure effect, we used C_{60} films thermally evaporated under ~10^{-6} Torr at 450 °C for 3 h 30 min (average thickness of 10 nm). Note that this condition provides an optimized C_{60} film thickness at which the vapor pressure effect is demonstrated most obviously in terms of growth direction,

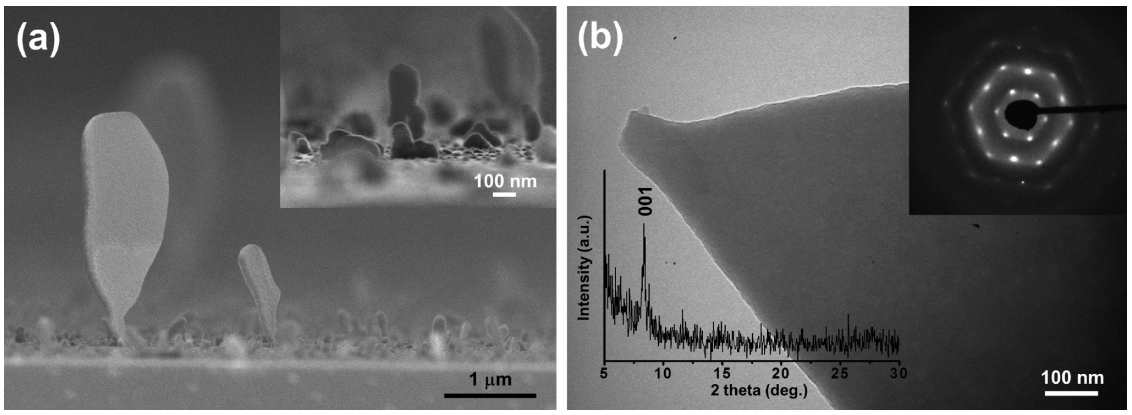

Figure 4. (a) SEM image of vertical C_{60} 2D disk structures with high magnification image (inset). (b) TEM image of a vertical C_{60} 2D disk with corresponding SAED pattern in inset (right). The inset on the left is the XRD pattern of vertically grown C_{60} 2D disks.

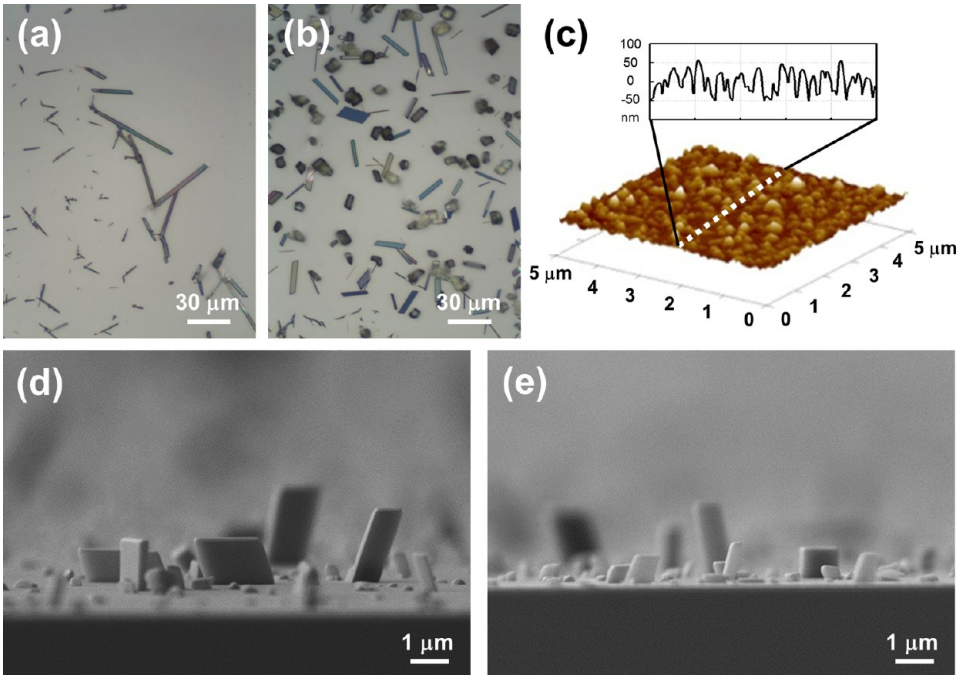

Figure 5. (a, b) Optical microscope images taken after drop-drying PT solutions in toluene and CH_2Cl_2, respectively. (c) AFM image of thermally evaporated PT film. (d, e) SEM images taken after running SVA processes using a sample in (c) with toluene and CH_2Cl_2, respectively.

density, length, and thickness of the resulting C_{60} nanowires depending on the types of solvent. Indeed, a high population of C_{60} dots with small numbers of laterally grown C_{60} nanowires is mainly observed when 1,3-dichlorobenzene is employed (Figure 3a), while mesitylene solvent yields vertical C_{60} nanowires of about 1 μm of length (Figure 3b). The C_{60} vertical nanowires grown by *m*-xylene under the same condition are much longer (Figure 3c). These results imply that solvent with higher vapor pressure provides a larger amount of solvent molecules guiding C_{60} molecules to crystallize in the vertical direction.

The above-mentioned results suggest that the direction of self-crystallization of organic molecules can be readily controlled under SVA conditions as long as the specific solvents guide the target molecules into meaningful geometrical structures, which can be easily screened by the drop-drying process. Hence, the versatility of the SVA process was examined for C_{60} again, but by switching the solvent from *m*-xylene to carbon tetrachloride (CCl_4, P_o = 114.0 mmHg at 25 °C), which is known to crystallize C_{60} molecules into lateral 2D disks by the drop-drying process.[11] When a C_{60} film is exposed to CCl_4 by the SVA process, C_{60} 2D disks are indeed formed in the vertical direction (Figure 4a and Figure S4; see also notes in the Figure S4 caption). The XRD and SAED results indicate that the crystals have a similar single-crystalline hexagonal crystal system to C_{60} 2D disks grown by the drop-drying process[11] (Figure 4b and Figure S5 in the Supporting Information).

The versatility of the SVA process was further shown with non-fullerene conjugated molecules, PT. When PT molecules dissolved in toluene (P_o = 28.4 mmHg at 25 °C)[38] and dichloromethane (CH_2Cl_2, P_o = 436.5 mmHg at 25 °C)[38] are applied for a regular drop-drying process, anisotropic PT anisotropic crystals are formed mainly at the coffee ring region of the droplets (Figure 5a and b, respectively), and the direction of PT anisotropic crystals is parallel to the substrate. On the other hand, when the SVA process is attempted using a substrate containing a thermally evaporated PT thin film (Figure 5c, average thickness of 60 nm), vertically grown PT anisotropic crystals are successfully obtained by the actions of both toluene and CH_2Cl_2 (Figure 5d and e, respectively). These results prove that the SVA process is a versatile growth methodology for the vertical formation of organic crystals.

CONCLUSION

In summary, we report a new methodology for the growth of vertical C_{60} 1D nanowires and 2D disks *via* crystallization of C_{60} molecules with the help of evaporating solvent molecules. While a conventional drop-drying of a C_{60} solution droplet in *m*-xylene generally results in laterally grown C_{60} nanowires owing to the dominant F_L over F_V applied to the solution droplet at the solid−liquid−air interface, the SVA process provides an ideal environment to enhance F_V, enforcing the crystallization of C_{60} molecules in the vertical direction. By switching the *m*-xylene solvent employed for the growth of vertical C_{60} nanowires to CCl_4, vertically grown C_{60} 2D disks are also obtained. The SVA process is further applied to other conjugated molecules, such as PT, which is also crystallized into vertical anisotropic crystals with the help of evaporating toluene or CH_2Cl_2. Considering the diversity of target molecules applicable for conjugated organic crystals, we believe that the SVA process with an appropriate selection of solvent is a versatile tool, opening a new direction of vertical growth of diverse organic and metal-containing organic nanostructures.

EXPERIMENTAL SECTION

Vertical Crystallization of C_{60} 1D Nanowires and 2D Disks. C_{60} fullerene powder was purchased (MTR Ltd., purity >99.95%) and used without further purification. For the vertical growth of C_{60} 1D nanowires, a C_{60} thin film was prepared by thermally evaporating C_{60} powder on a precleaned Si substrate under ~10^{-7} Torr at 540 °C for 7 h (average thickness of 60 nm). The precleaned Si substrate was prepared by rinsing with deionized water followed by rinsing with acetone and isopropyl alcohol, then blowing with N_2 gas. For the examination of the solvent effect shown in Figure 3, we used C_{60} films that were thermally evaporated under ~10^{-6} Torr at 450 °C for 3 h 30 min (average thickness of 10 nm). Temperature and evaporation time were varied to form C_{60} films of various thicknesses. The prepared C_{60} film samples were brought into a scintillation vial (70 mL) in which 5 mL of carrier solvent, such as *m*-xylene (Sigma-Aldrich, 99%), CCl_4 (Sigma-Aldrich, 99.9%), mesitylene (Sigma-Aldrich, 98%), and 1,3-dichlorobenzene (Aldrich, 98%), was preloaded. To avoid direct contact between the C_{60} film sample and solvent, another, smaller scintillation vial (20 mL) pillar was placed inside the vial on which the C_{60} film sample was placed. Then the vial was capped to trap solvent vapors inside the vial and placed in an oven preset at 28 °C. Various reaction times were examined, and the optimized reaction time was determined to be 12 h. Once the reaction was completed, the C_{60} film sample was carefully taken out of the vial, then left in air for 6 h to completely dry off the solvents from the samples.

Vertical Crystallization of 5,7,12,14-Pentacenetetrone Anisotropic Crystals. For the test of the drop-drying process, a saturated PT solution was prepared by adding an excess amount of PT in toluene (Fisher Scientific, HPLC grade) and CH_2Cl_2 (Fisher Scientific, HPLC grade) followed by ultrasonicating and filtrating (Whatman International Ltd., pore size <20 nm) the precipitates. For filtering solutions, we used an inorganic membrane filter. An aliquot (about 5 μL) of the saturated PT solution was dropped on a precleaned Si substrate in air at room temperature. The formation of PT anisotropic crystals laying down on a substrate was confirmed using an optical microscope. For the vertical growth of PT anisotropic crystals, a PT thin film was prepared on a Si substrate by thermal evaporation (3×10^{-6} Torr at 300 °C for 30 min), then placed inside a scintillation vial filled with toluene or CH_2Cl_2, as in the case of C_{60} vertical growth, and kept for 24 h at 28 °C. Once the reaction was completed, the PT film sample was carefully taken out of the vial, then left in air for 6 h to completely dry off the solvents from the sample.

Structure Characterization. C_{60} film morphology was investigated by a tapping mode atomic force microscope (AFM, Nanoscope IIIa, Digital Instrument Inc.). The morphologies of all the products were examined by scanning electron microscopy (SEM, JEOL, JSM-7410F) with an ultrathin (~10 Å) Pt coating. Structural information was obtained by transmission electron microscopy (TEM, Carl Zeiss, EM 912 omega), area selective electron diffraction (SAED, and powder X-ray diffraction (XRD) for a single C_{60} nanowire. We prepared a single C_{60} nanowire on a Cu grid (Ted Pella, Inc., 400 mesh) by mildly sliding a Cu grid on as-grown wires on a Si substrate for TEM analysis. X-ray diffraction data were obtained from the 5D beamline at Pohang Accelerator Laboratory (λ = 1.2390 Å). All obtained data were converted to Cu Kα (λ = 1.54057 Å) radiation scale for convenience in comparing with previously reported data. To determine the solvation of vertical C_{60} nanowires, Raman spectra were acquired by using a Raman spectroscope (Alpha 300R, WITEC) equipped with a 532 nm diode laser (power = 0.1 mW, grating = 1800 g/mm, BLZ = 500 nm).

Conflict of Interest: The authors declare no competing financial interest.

Supporting Information Available: Optical microscope images, SAED with TEM images, XRD, movie clip data for C_{60} nanostructures obtained by drop-drying a C_{60} solution, low-magnification SEM image of a vertically grown C_{60} 2D disk, coffee ring effect upon drop-drying process depending on the droplet size. This material is available free of charge *via* the Internet at http://pubs.acs.org.

Acknowledgment. This work was supported by a National Research Foundation of Korea (NRF) grant funded by Ministry of Science, ICT & Future Planning (2012R1A2A1A01003040, 2013K1-A3A1A32035430, NRF-2013M3C1A3041869). We acknowledge the use of the 5D beamline at Pohang Accelerator Laboratory (PAL) and TEM at Korea Basic Science Institute (KBSI).

REFERENCES AND NOTES

1. Mas-Torrent, M.; Rovira, C. Role of Molecular Order and Solid-State Structure in Organic Field-Effect Transistors. *Chem. Rev.* **2011**, *111*, 4833–4856.

2. Da Como, E.; Loi, M. A.; Murgia, M.; Zamboni, R.; Muccini, M. J-Aggregation in α-Sexithiophene Submonolayer Films on Silicon Dioxide. *J. Am. Chem. Soc.* **2006**, *128*, 4277–4281.
3. Sundar, V. C.; Zaumseil, J.; Podzorov, V.; Menard, E.; Willett, R. L.; Someya, T.; Gershenson, M. E.; Rogers, J. A. Elastomeric Transistor Stamps: Reversible Probing of Charge Transport in Organic Crystals. *Science* **2004**, *303*, 1644–1646.
4. Park, J. E.; Son, M.; Hong, M.; Lee, G.; Choi, H. C. Crystal-Plane-Dependent Photoluminescence of Pentacene 1D Wire and 2D Disk Crystals. *Angew. Chem., Int. Ed.* **2012**, *51*, 6383–6388.
5. Yoon, S. M.; Lee, J.; Je, J. H.; Choi, H. C.; Yoon, M. Optical Waveguiding and Lasing Action in Porphyrin Rectangular Microtube with Subwavelength Wall Thicknesses. *ACS Nano* **2011**, *5*, 2923–2929.
6. Woo, H. Y.; Liu, B.; Kohler, B.; Korystov, D.; Mikhailovsky, A.; Bazan, G. C. Solvent Effects on the Two-Photon Absorption of Distyrylbenzene Chromophores. *J. Am. Chem. Soc.* **2005**, *127*, 14721–14729.
7. Miyazawa, K.; Kuwasaki, Y.; Obayashi, A.; Kuwabara, M. C_{60} Nanowhiskers Formed by the Liquid-Liquid Interfacial Precipitation Method. *J. Mater. Res.* **2002**, *17*, 83–88.
8. Dong, A.; Chen, J.; Vora, P. M.; Kikkawa, J. M.; Murray, C. B. Binary Nanocrystal Superlattice Membranes Self-Assembled at the Liquid-Air Interface. *Nature* **2010**, *466*, 474–477.
9. Li, H.; Tee, B. C.-K.; Cha, J. J.; Cui, Y.; Chung, J. W.; Lee, S. Y.; Bao, Z. High-Mobility Field-Effect Transistors from Large-Area Solution-Grown Aligned C_{60} Single Crystals. *J. Am. Chem. Soc.* **2012**, *134*, 2760–2765.
10. Zhang, C.; Zhang, X.; Zhang, X.; Fan, X.; Jie, J.; Chang, J. C.; Lee, C.-S.; Zhang, W.; Lee, S.-T. Facile One-Step Growth and Patterning of Aligned Squaraine Nanowires *via* Evaporation-Induced Self-Assembly. *Adv. Mater.* **2008**, *20*, 1716–1720.
11. Park, C.; Song, H. J.; Choi, H. C. The Critical Effect of Solvent Geometry on the Determination of Fullerene (C_{60}) Self-Assembly into Dot, Wire and Disk Structures. *Chem. Commun.* **2009**, 4803–4805.
12. Reches, M.; Gazit, E. Controlled Patterning of Aligned Self-Assembled Peptide Nanotubes. *Nat. Nanotechnol.* **2006**, *1*, 195–200.
13. Ryu, J.; Park, C. B. High-Temperature Self-Assembly of Peptides into Vertically Well-Aligned Nanowires by Aniline Vapor. *Adv. Mater.* **2008**, *20*, 3754–3758.
14. Xu, X.-D.; Wang, X.-G.; Lin, B.-B.; Cheng, H.; Zhang, X.-Z.; Zhuo, R.-X. Interface Self-Assembly to Construct Vertical Peptide Nanorods on Quartz Template. *Chem. Commun.* **2011**, *47*, 7113–7115.
15. Adler-Abramovich, L.; Aronov, D.; Beker, P.; Yevnin, M.; Stempler, S.; Buzhansky, L.; Rosenman, G.; Gazit, E. Self-Assembled Arrays of Peptide Nanotubes by Vapour Deposition. *Nat. Nanotechnol.* **2009**, *4*, 849–854.
16. Ryu, J.; Park, C. B. Solid-Phase Growth of Nanostructures from Amorphous Peptide Thin Film: Effect of Water Activity and Temperature. *Chem. Mater.* **2008**, *20*, 4284–4290.
17. Huang, K.-J.; Hsiao, Y.-S.; Whang, W.-T. Low-Temperature Formation of Self-Assembled 1,5-Diaminoanthraquinone Nanofibers: Substrate Effects and Field Emission Characteristics. *Org. Electron.* **2011**, *12*, 686–693.
18. Zhao, Y. S.; Zhan, P.; Kim, J.; Sun, C.; Huang, J. Patterned Growth of Vertically Aligned Organic Nanowire Waveguide Arrays. *ACS Nano* **2010**, *4*, 1630–1636.
19. Zhao, Y. S.; Wu, J.; Huang, J. Vertical Organic Nanowire Arrays: Controlled Synthesis and Chemical Sensors. *J. Am. Chem. Soc.* **2009**, *131*, 3158–3159.
20. Yang, F.; Shtein, M.; Forrest, S. R. Controlled Growth of a Molecular Bulk Heterojunction Photovoltaic Cell. *Nat. Mater.* **2005**, *4*, 37–41.
21. Zhou, Y.; Zhou, W. Growth Mechanism of C_{60}/Mesitylene Nanowires. *CrystEngComm* **2012**, *14*, 1449–1454.
22. Kim, S. H.; Misner, M. J.; Russell, T. P. Solvent-Induced Ordering in Thin Film Diblock Copolymer/Homopolymer Mixtures. *Adv. Mater.* **2004**, *16*, 2119–2123.
23. Xuan, Y.; Peng, J.; Cui, L.; Wang, H.; Li, B.; Han, Y. Morphology Development of Ultrathin Symmetric Diblock Copolymer Film *via* Solvent Vapor Treatment. *Macromolecules* **2003**, *37*, 7301–7307.
24. De Luca, G.; Treossi, E.; Liscio, A.; Mativetsky, J. M.; Scolaro, L. M.; Palermo, V.; Samorì, P. Solvent Vapour Annealing of Organic Thin Films: Controlling the Self-Assembly of Functional Systems across Multiple Length Scales. *J. Mater. Chem.* **2010**, *20*, 2493–2498.
25. Ding, Z.; Xing, R.; Zheng, L.; Sun, Y.; Wang, X.; Ding, J.; Wang, L.; Han, Y. Self-Assembly of Carbazole-Based Dendrimers by Solvent Vapor Annealing: From Fibers to Spherulites. *J. Phys. Chem. B* **2011**, *115*, 15159–15166.
26. Lu, G.; Li, L.; Yang, X. Creating a Uniform Distribution of Fullerene C_{60} Nanorods in a Polymer Matrix and Its Photovoltaic Applications. *Small* **2008**, *4*, 601–606.
27. Wang, L.; Liu, B.; Liu, D.; Yao, M.; Hou, Y.; Yu, S.; Cui, T.; Li, D.; Zou, G.; Iwasiewicz, A.; *et al*. Synthesis of Thin, Rectangular C_{60} Nanorods Using *m*-Xylene as a Shape Controller. *Adv. Mater.* **2006**, *18*, 1883–1888.
28. Wang, L.; Liu, B.; Yu, S.; Yao, M.; Liu, D.; Hou, Y.; Cui, T.; Zou, G.; Sundqvist, B.; You, H.; *et al*. Highly Enhanced Luminescence from Single-Crystalline $C_{60}\cdot 1m$-Xylene Nanorods. *Chem. Mater.* **2006**, *18*, 4190–4194.
29. Talyzin, A.; Jansson, U. C_{60} and C_{70} Solvates Studied by Raman Spectroscopy. *J. Phys. Chem. B* **2000**, *104*, 5064–5071.
30. Minato, J.-I.; Miyazawa, K. Solvated Structure of C_{60} Nanowhiskers. *Carbon* **2005**, *43*, 2837–2841.
31. Ramm, M.; Luger, P.; Zobel, D.; Duczek, W.; Boeyens, J. C. A. Static Disorder in Hexagonal Crystal Structures of C_{60} at 100 and 20 K. *Cryst. Res. Technol.* **1996**, *31*, 43–53.
32. Simulations were performed using a CrystalMaker software package: *CrystalMaker 2.1.4*, *CrystalDiffract 1.2.2*, *SingleCrystal 1.1.3*; CrystalMaker Software Ltd., Oxford, England, 2009.
33. Deegan, R. D.; Bakajin, O.; Dupont, T. F.; Huber, G.; Nagel, S. R.; Witten, T. A. Capillary Flow as the Cause of Ring Stains from Dried Liquid Drops. *Nature* **1997**, *389*, 827–829.
34. Sear, R. P. Nucleation at Contact Lines where Fluid-Fluid Interfaces Meet Solid Surfaces. *J. Phys.: Condens. Matter* **2007**, *19*, 466106.
35. Li, K.; Xu, S.; Shi, W.; He, M.; Li, H.; Li, S.; Zhou, X.; Wang, J.; Song, Y. Investigating the Effects of Solid Surfaces on Ice Nucleation. *Langmuir* **2012**, *28*, 10749–10754.
36. Kassel, L. S. Vapor Pressures of the Xylenes and Mesitylene. *J. Am. Chem. Soc.* **1936**, *58*, 670–671.
37. Dreisbach, R. R.; Shrader, S. A. Vapor Pressure-Temperature Data on Some Organic Compounds. *Ind. Eng. Chem.* **1949**, *41*, 2879–2880.
38. *CRC Handbook of Chemistry and Physics*, 84th ed.; CRC: New York, 2003; pp 2266−2269.